Strong-field photoionization and emission of light in the wave-packet-spreading regime

M. V. Fedorov and J. Peatross
General Physics Institute, Russian Academy of Sciences, 38 Vavilov Street, Moscow 117942, Russia
(Received 19 September 1994)

Barrier suppression ionization and wave-packet-spreading models are used to describe to first order in a perturbative expansion the quantum-mechanical interaction between a photodetached electron wave packet and its parent nucleus in the presence of a very strong laser field. The attraction between the wave packet and the nucleus (the first-order approximation to the dipole acceleration) is interpreted in terms of a force arising from an effective potential, where the effective potential is defined to attract the electron treated as a point particle by the same amount that the true Coulomb potential attracts the spreading wave packet. Thus the effective potential has no Coulomb singularity at the origin. The obtained expression for dipole acceleration is used to calculate the emission spectrum of the detached wave packet interacting in the strong laser field with the nucleus. In the case of detachment of the hydrogen ground-state wave packet, the spectrum is shown to be broad and almost completely devoid of definite harmonics of the laser frequency. The lack of any pronounced structure in the emission spectrum is explained by rapid spreading of the electron wave packet and by the resulting strong smoothing of the effective interaction potential and force. The limitations on the applicability of the presented theory are discussed and are shown to be rather stringent: the laser pulse must be very short (a few optical cycles) and very strong (of the order of the atomic field).

PACS number(s): 32.80.Rm, 32.80.Fb

I. INTRODUCTION

Photoionization of atoms by a strong and superstrong light field is a subject of rather wide interest, both experimental and theoretical. Many theoretical models have been suggested to describe this process as well as accompanying phenomena, such as the emission of harmonics of the laser field. The applicability of the various models depends strongly on the parameters of laser radiation: its intensity, frequency, and pulse duration. Two models of importance to the topic of this paper are the barrier suppression ionization (BSI) [1] and wave-packet-spreading (WPS) [2–5] models. In the BSI picture, ionization is assumed to occur suddenly and completely when the height of the atomic potential barrier is suppressed by the laser field past the level of the electron binding potential. In this paper, we assume further that the wave packet of the bound state remains undistorted until the moment of ionization. The WPS model assumes that once the electronic wave packet has been released from the atom, it spreads quantum mechanically in the laser field while remaining almost free from an influence of the atomic potential. The main assumptions of the BSI and WPS models are further explained in Sec. II.

On an intuitive level, the main result of this work can be formulated in advance as follows: From the BSI-WPS assumptions, once the light field $\varepsilon(t)$ becomes strong enough to release the originally bound electron, the "center of mass" of the electron wave packet follows a classical electron trajectory $\mathbf{r}_{\rm cl}(t)$ in the laser field, whereas the electron charge distribution density spreads quantum mechanically. Spreading is characterized by the function $\psi(\mathbf{r},t)$ of an electron free from both the Coulomb and light fields. Under the BSI-WPS assumptions, the electron charge distribution density is proportional to $|\psi(\mathbf{r};t)|^2$, which is centered on the classical trajectory. The attraction between the nucleus and the spreading and oscillating electron wave packet may be found through a direct application of Coulomb's law. The attraction (effective force) between the nucleus and the wave packet is given by a superposition of $\mathbf{F}_{\rm Coul}(\mathbf{r})$ with the weight function $|\psi(\mathbf{r};t)|^2$:

$$\mathbf{F}_{\rm eff}(t)=\int d\mathbf{r}'\mathbf{F}_{\rm Coul}(\mathbf{r}+\mathbf{r}')|\psi(\mathbf{r}';t)|^2|_{\mathbf{r}=\mathbf{r}_{\rm cl}(t)} . \quad (1)$$

As can be easily understood, the quantum-mechanical spreading reduces the force on the electron cloud since more of the wave packet becomes situated further from the nucleus. Below in Sec. III, Eq. (1) is rigorously shown to be valid in the first order of the quantum-mechanical perturbation theory based on an expansion with respect to the interaction of the detached electron with its parent nucleus. The results of the quantum-mechanical derivation are further compared with a classical picture and interpreted in terms of the effective atomic potential and force. Specific calculations of the effective force and potential are presented and discussed in Sec. IV. In Sec. V, emission of light by the detached electron in the very strong laser field is examined, and the fast spreading of the wave packet is seen to strongly suppress harmonic production. The main limitations of the present approach, which are rather stringent, are discussed in Sec. VI.

II. BSI AND WPS MODELS

In the hydrogen atom, the total potential energy U of the electron is given by a sum of the Coulomb energy

$-1/|\mathbf{r}|$, and the energy of electron-light interaction $\mathbf{r}\cdot\boldsymbol{\varepsilon}(t)$, where $\boldsymbol{\varepsilon}(t)$ is the electric component of the light field

$$\boldsymbol{\varepsilon}(t)=\boldsymbol{\varepsilon}_0(t)\cos(\omega t) . \tag{2}$$

Here $\boldsymbol{\varepsilon}_0(t)$ is the time-dependent amplitude envelope and ω is the light frequency. Atomic units ($\hbar=m=|e|=1, e_{el}=-1$) are used throughout the paper. The total electron potential energy U is plotted in Fig. 1 as a function of $x=\mathbf{r}\cdot\boldsymbol{\varepsilon}(t)/|\boldsymbol{\varepsilon}(t)|$. The curve $U(x)$ has a form of a potential barrier with a height $U_{max}=-2\sqrt{|\boldsymbol{\varepsilon}(t)|}$. If the barrier is lower than the field-free atomic ground-state level E_0, $U_{max}<E_0=-1/2$, the electron can freely leave the atom by propagating above the barrier. In other words, ionization occurs when the laser field effectively suppresses the barrier to the electron motion, which is the main assumption of the BSI model. The formulated BSI condition ($U_{max}<E_0$) can be rewritten as

$$|\boldsymbol{\varepsilon}(t)|>1/16 . \tag{3}$$

This equation may be interpreted as an equation for t, i.e., for that instant of time during the light pulse when a growing and oscillating field $\boldsymbol{\varepsilon}(t)$ [Eq. (2)] first achieves a strength sufficient for the BSI condition (3) to be fulfilled. Usually this instant of time occurs near an oscillation peak of $\boldsymbol{\varepsilon}(t)$ [when $\cos(\omega t)=1$ or -1]. Let $t=0$ correspond to the position of the first oscillation peak for which the BSI condition is fulfilled. Rigorously, the BSI condition [Eq. (2)] can first be met at some time $t_0\neq 0$ between peaks of the growing and oscillating field $\boldsymbol{\varepsilon}(t)$, especially for very short pulses. For simplicity, we will adopt the convention $t_0=0$. Then according to the BSI assumption, before $t=0$ the field is too weak to produce significant ionization, whereas after $t=0$ the above-barrier ionization is very fast and almost complete, and occurs during a period of time much shorter than the spacing π/ω between neighboring peaks of the field $\boldsymbol{\varepsilon}(t)$.

As an extension of the ideas of BSI, we can assume that once the electron is released from the atom, its wave packet freely spreads as it is driven by a strong laser field. This is the assumption of the WPS model. As mentioned above the center of mass of such a wave packet follows the trajectory of a classical dot-particle in the field $\boldsymbol{\varepsilon}(t)$, $\mathbf{r}_{cl}(t)$, i.e., it oscillates with the amplitude equal to $\alpha_0(t)=\boldsymbol{\varepsilon}_0(t)/\omega^2$. The WPS assumption of electron motion that is almost free from the atomic potential is only applicable if the free-electron quiver motion amplitude a_0 is much larger than the initial atomic size, i.e, if

$$\alpha_0(0)=\boldsymbol{\varepsilon}_0(0)/\omega^2\gg 1 . \tag{4}$$

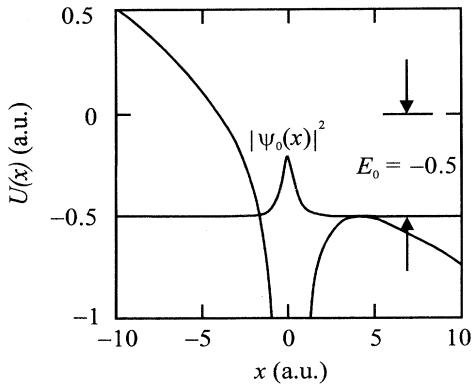

FIG. 1. The atomic electron potential energy in the presence of an electric field $\varepsilon=1/16$. The hydrogen $1s$ state probability density is also depicted, and the height of the barrier has been suppressed to $E_0=-1/2$ a.u., the $1s$ state binding energy.

Theoretically, the BSI-WPS conditions imply the following formulation of the problem to be solved. Before the BSI instant of time $t=0$ the atom is stable, and the electron wave function for $t<0$ is $\Psi(\mathbf{r},t)=\psi_0(\mathbf{r})\exp(-iE_0t)$ where $\psi_0(\mathbf{r})$ is the field-free ground-state atomic wave function. After the BSI instant of time $t=0$, the electron is free from the atomic potential, and the wave function $\Psi(\mathbf{r},t)$ obeys the Schrödinger equation in the field $\boldsymbol{\varepsilon}(t)$ in the absence of the atomic potential, and with the initial condition $\Psi(\mathbf{r},0)=\psi_0(\mathbf{r})$. This is an approximation in which no residual nucleus-electron interaction is taken into account at all. Such a problem has been solved in Ref. [5], where the expression for the wave function was projected upon the ground-state wave function. The results were compared with exact *ab-initio* calculations, i.e., with numerical solutions of the exact Schrödinger equation in which both the light field $\boldsymbol{\varepsilon}(t)$ and a one-dimensional (1D) model atomic potential were taken into account. Similar exact numerical solutions for different model atomic potentials and different laser pulse envelopes were investigated in Ref. [6]. In this paper, the analytical calculations of Ref. [5] will be extended to take into account the interaction of the detached electron wave packet with its parent nucleus in a first-order approximation. Further, the emission that can occur due to this first-order correction will be examined.

It should be mentioned that in some sense the BSI-WPS model is complementary to the well-known Keldysh-Faisal-Reiss (KFR) approach [7–9], known also as the theory of optical tunneling. In our opinion, the difference between these two models originates from a rather fundamental difference between the below- and above-threshold propagation of the detached electron, i.e., between tunneling and barrier-suppression. This difference implies a rather significant difference in the theories of light emission in the BSI-WPS regime (Sec. V of this paper) and in the KFR [11] regime, below the BSI threshold.

Finally, it should be mentioned that in order for the BSI-WPS model to be valid, the pulse duration τ must be constrained [5] by the condition that the width of the spreading free-electron wave packet [see Eqs. (27), (34) below] remains smaller than $2\alpha_0$. Otherwise the atomic potential begins playing a much more important role by forming stationary Kramers-Henneberger bound states [10].

III. THE FIRST-ORDER DIPOLE ACCELERATION

A. Quantum-mechanical derivation

We begin from the general nonstationary Schrödinger equation for the electron influenced by both the Coulomb

and laser fields

$$i\partial\Psi(\mathbf{r},t)/\partial t=[-\tfrac{1}{2}\partial^2/\partial\mathbf{r}^2+V(\mathbf{r})+\mathbf{r}\cdot\boldsymbol{\varepsilon}(t)]\Psi(\mathbf{r},t)\ , \tag{5}$$

where $V(\mathbf{r})$ is the atomic potential, which for the hydrogen atom is $-1/|\mathbf{r}|$. In accordance with the main BSI-WPS assumptions discussed above by neglecting $V(\mathbf{r})$ we can find immediately the following approximate solution of Eq. (5) valid in the region $t>0$:

$$\Psi^{(0)}(\mathbf{r},t)=\int d\mathbf{r}'U_V(\mathbf{r},t;\mathbf{r}',0)\psi_0(\mathbf{r}')\ , \tag{6}$$

where $U_V(\mathbf{r},t;\mathbf{r}',t')$ is the Volkov evolution operator that can be expressed in terms of the nonrelativistic Volkov functions $\Psi_{\mathbf{p}}^V(\mathbf{r},t)$

$$U_V(\mathbf{r},t;\mathbf{r}',t')=\int d\mathbf{p}\Psi_{\mathbf{p}}^V(\mathbf{r},t)[\Psi_{\mathbf{p}}^V(\mathbf{r}',t')]^*\ . \tag{7}$$

The nonrelativistic Volkov functions are known to be given by

$$\Psi_{\mathbf{p}}^V(\mathbf{r},t)=\frac{1}{(2\pi)^{3/2}}\times\exp\left\{i\mathbf{p}\mathbf{r}-\frac{i}{2}\int_0^t dt'\left[\mathbf{p}+\frac{\mathbf{A}(t')}{c}\right]^2\right\}\ , \tag{8}$$

where $\mathbf{A}(t)=-c\int_0^t dt'\boldsymbol{\varepsilon}(t')$ is the vector potential of the laser field and c is the speed of light ($c=137$ in atomic units). The nonrelativistic Volkov function $\Psi_{\mathbf{p}}^V(\mathbf{r},t)$ and the evolution operator $U_V(\mathbf{r},t;\mathbf{r}',t')$, and hence also $\Psi^{(0)}(\mathbf{r},t)$ of Eq. (6), obey the Schrödinger equation [Eq. (5)] in the absence of the atomic potential $V(\mathbf{r})$. $\Psi^{(0)}(\mathbf{r},t)$ obeys the necessary initial condition since $U_V(\mathbf{r},t;\mathbf{r}',t)=\delta(\mathbf{r}-\mathbf{r}')$, which gives $\Psi^{(0)}(\mathbf{r},0)=\psi_0(\mathbf{r})$.

It will be convenient occasionally to employ a symbolic notation for Eqs. (6) and (7) (as well as for some other arising equations) by dropping the coordinate variables $\mathbf{r}$ and $\mathbf{r}'$. In the symbolic notation $\hat{U}_V(t;t)=1$, and Eqs. (6) and (7) are written as

$$|\Psi^{(0)}(t)\rangle=\hat{U}_V(t;0)|\Psi(0)\rangle\ ,$$
$$\hat{U}_V(t;t')=\int d\mathbf{p}|\Psi_{\mathbf{p}}^V(t)\rangle\langle\Psi_{\mathbf{p}}^V(t')|. \tag{9}$$

Some other useful features of the evolution operator are

$$[\hat{U}_V(t;t')]^\dagger=\hat{U}_V(t';t),$$
$$i\frac{\partial}{\partial t}\hat{U}_V(t;t')=H_0(t)\hat{U}_V(t;t'),$$
$$i\frac{\partial}{\partial t}\hat{U}_V(t';t)=-\hat{U}_V(t;t')H_0(t')\ , \tag{10}$$

where $H_0(t)=\frac{1}{2}[\hat{\mathbf{p}}+(1/c)\mathbf{A}(t)]^2$ and $\hat{\mathbf{p}}=-i\nabla$.

From Eqs. (6)–(9) the zeroth order (with respect to the atomic potential, i.e., the atomic potential completely omitted) average dipole moment and dipole acceleration are found to be

$$\mathbf{d}^{(0)}(t)=-\langle\Psi^{(0)}(t)|\mathbf{r}|\Psi^{(0)}(t)\rangle=-\frac{1}{c}\int_0^t dt'\mathbf{A}(t')\ ,$$
$$\ddot{\mathbf{d}}^{(0)}(t)=\boldsymbol{\varepsilon}(t)\ . \tag{11}$$

These equations are identical to the Newton equation for a classical charged particle in the field $\boldsymbol{\varepsilon}(t)$. This means that in the zeroth-order approximation the quantum-mechanical and classical descriptions of the electron motion are the same. It should be noted that no harmonics of the laser field appear in Eq. (11); $\ddot{\mathbf{d}}^{(0)}(t)$ describes only the well-known Rayleigh scattering, i.e, light scattering without any frequency change.

We now turn our attention to the first-order corrections to the dipole arising from the residual electron-nucleus interaction. This means that we have to find a correction $\Psi^{(1)}(\mathbf{r},t)$ to $\Psi^{(0)}(\mathbf{r},t)$ of Eq. (6) by considering now $V(\mathbf{r})$ in Eq. (5) as a small perturbation. The first-order wave function $\Psi^{(1)}(\mathbf{r},t)$ can be written as a superposition of the nonrelativistic Volkov wave functions $\Psi_{\mathbf{p}}^V(\mathbf{r},t)$ [Eq. (8)] with some unknown coefficients $C_{\mathbf{p}}(t)$. Equations for $C_{\mathbf{p}}(t)$ follow directly from the Schrödinger equation [Eq. (5)] by inserting $\Psi^{(0)}(\mathbf{r},t)+\Psi^{(1)}(\mathbf{r},t)$ into both sides of the Schrödinger equation while ignoring the term $\Psi^{(1)}(\mathbf{r},t)V(\mathbf{r})$. Without dwelling upon the details of this solution, which are straightforward, let us write down the resulting expression for the first-order wave function in the symbolic form that employs the evolution operator defined in Eqs. (7) and (9)

$$|\Psi^{(1)}(t)\rangle=-i\int_0^t dt'\hat{U}_V(t;t')V\hat{U}_V(t';0)|\psi_0\rangle\ . \tag{12}$$

From this equation we can also find the first-order correction to the dipole moment

$$\mathbf{d}^{(1)}(t)=-[\langle\Psi^{(1)}(t)|\mathbf{r}|\Psi^{(0)}(t)\rangle+\langle\Psi^{(0)}(t)|\mathbf{r}|\Psi^{(1)}(t)\rangle]$$
$$=i\int_0^t dt'\langle\psi_0|\hat{U}_V(0;t)\mathbf{r}\hat{U}_V(t;t')\times V\hat{U}_V(t';0)|\psi_0\rangle+\text{c.c.} \tag{13}$$

The second derivative of $\mathbf{d}^{(1)}(t)$ determines the dipole acceleration calculated for the first-order approximation. In calculating $\ddot{\mathbf{d}}^{(1)}(t)$ it is helpful to take into account the features of the evolution operator $\hat{U}_V(t;t')$ indicated in Eq. (10) as well as the commutation rules: $[H_0(t),\mathbf{r}]=-i[\hat{\mathbf{p}}+(1/c)\mathbf{A}(t)]$ and $[H_0(t),\hat{\mathbf{p}}]=0$. Then $\ddot{\mathbf{d}}^{(1)}(t)$ can be reduced to the form

$$\ddot{\mathbf{d}}^{(1)}(t)=2\text{Re}\{i\langle\psi_0|\hat{U}_V(0;t)\hat{\mathbf{p}}V\hat{U}_V(t;0)|\psi_0\rangle\}\ . \tag{14}$$

B. Classical picture

For a clearer interpretation, the quantum-mechanical perturbation theory described above can be compared with the corresponding iteration procedure in a classical picture. The exact classical Newton equation for a charged particle (electron) influenced by the atomic potential and the light field has a form

$$\ddot{\mathbf{r}}=-\boldsymbol{\varepsilon}(t)-\nabla V(\mathbf{r})\ . \tag{15}$$

If we assume that the role of the atomic force is small as compared to $\boldsymbol{\varepsilon}(t)$ we can use an iteration method to solve Eq. (15) similar to the one used above. Under this assumption the solution of Eq. (15) is represented in the form of a series

$$\mathbf{r}(t)=\mathbf{r}^{(0)}(t)+\mathbf{r}^{(1)}(t)+\cdots\ ,$$
$$V(\mathbf{r}(t))=V(\mathbf{r}^{(0)}(t))+\mathbf{r}^{(1)}(t)\cdot\nabla V(\mathbf{r})|_{\mathbf{r}=\mathbf{r}^{(0)}(t)}+\cdots\ , \tag{16}$$

where $\mathbf{r}^{(n)}(t)\sim[V(\mathbf{r})]^n$. By substituting these expansions into Eq. (15) and by retaining only the terms of the same order of magnitude (of the zeroth, first order in V, etc.) we arrive, in particular, at equations of the zeroth and first order

$$\mathbf{r}^{(0)}(t)=\frac{1}{c}\int_0^t dt'\,\mathbf{A}(t')\ ,$$
$$\ddot{\mathbf{r}}^{(1)}(t)=-\nabla V(\mathbf{r})|_{\mathbf{r}=\mathbf{r}^{(0)}(t)}\ . \tag{17}$$

The first of Eqs. (17) is equivalent to the first of Eqs. (11). From the second of Eqs. (17) the classical first-order dipole acceleration can be determined

$$\ddot{\mathbf{d}}_{\rm cl}^{(1)}(t)=\nabla V(\mathbf{r})|_{\mathbf{r}=\mathbf{r}^{(0)}(t)}\ . \tag{18}$$

C. Effective potential and force

We now compare the quantum-mechanical and classical expressions for the first-order dipole acceleration [Eqs. (14) and (18)]. In fact, it can be shown that the quantum-mechanical expression for the dipole acceleration of Eq. (14) can be reduced to a form similar to that of Eq. (18)

$$\ddot{\mathbf{d}}^{(1)}(t)=\nabla V_{\rm eff}(\mathbf{r};t)|_{\mathbf{r}=\mathbf{r}^{(0)}(t)}=-\mathbf{F}_{\rm eff}(t)\ , \tag{19}$$

where $\mathbf{F}_{\rm eff}(t)$ is the effective force of Eq. (1) and $V_{\rm eff}(\mathbf{r};t)$ is the corresponding effective potential

$$V_{\rm eff}(\mathbf{r};t)=\int d\mathbf{r}'V(\mathbf{r}+\mathbf{r}')|\psi(\mathbf{r}';t)|^2\ . \tag{20}$$

Here $\psi(\mathbf{r};t)$ is the free-electron wave function that obeys the Schrödinger equation [Eq. (5)] in the absence of both the $V(\mathbf{r})$ and the $\mathbf{r}\cdot\boldsymbol{\varepsilon}(t)$ terms, and which obeys the initial condition $\psi(\mathbf{r};0)=\psi_0(\mathbf{r})$. In this case, $\psi(\mathbf{r};t)$ is neither affected by the atomic potential nor by the laser field, and depends on time t only through the quantum-mechanical spreading of the initial wave packet. Explicitly, $\psi(\mathbf{r};t)$ is given by

$$\psi(\mathbf{r};t)=\frac{1}{(2\pi)^3}\int d\mathbf{p}\int d\mathbf{r}'\exp\left[i\mathbf{p}(\mathbf{r}-\mathbf{r}')-\frac{ip^2t}{2}\right]\psi_0(\mathbf{r}')$$
$$=\left[\frac{-i}{2\pi t}\right]^{3/2}\int d\mathbf{r}'\exp\left[i\frac{(\mathbf{r}-\mathbf{r}')^2}{2t}\right]\psi_0(\mathbf{r}')\ . \tag{21}$$

A qualitative interpretation of these results is very simple. The difference between $V_{\rm eff}(\mathbf{r};t)$ of Eq. (20) and $V(\mathbf{r})$ arises because in quantum mechanics, the electron is a cloud rather than a point. The density of the electron distribution in space is given by $|\psi(\mathbf{r}';t)|^2$, and the bare atomic potential $V(\mathbf{r})$ must be averaged with this weight function in order to get the effective potential of Eq. (20). The term $\mathbf{r}$ in the argument of the effective potential in Eq. (20) is interpreted as the vector determining a position of the center of mass of the electron cloud, or wave packet. Owing to spreading, both the electron distribution and the effective atomic potential depend on time t. Perhaps, the most interesting aspect of the results derived [Eqs. (1), (19), and (20)] is the separation of the effects arising from the quantum-mechanical spreading and from the classical oscillations of the electron in the laser field $\boldsymbol{\varepsilon}(t)$. In accordance with Eqs. (20) and (21), to calculate the average quantum-mechanical dipole acceleration in the first-order approximation, one can first solve the WPS problem for the field-free electron. Then the classical electron trajectory $\mathbf{r}^{(0)}(t)$ in the laser field $\boldsymbol{\varepsilon}(t)$ replaces $\mathbf{r}$ in the field-free effective force $-\nabla V_{\rm eff}(\mathbf{r};t)$. Thus, there are two independent effects that cause the average quantum-mechanical dipole acceleration [Eq. (19)] to depend on time t. These are (i) the dependence on t via the effective potential itself arising from the WPS and (ii) the dependence on t via the classical electron quiver motion or the positioning of the wave packet center of mass as specified when $\mathbf{r}^{(0)}(t)$ is substituted into $-\nabla V_{\rm eff}(\mathbf{r};t)$ instead of $\mathbf{r}$.

The three-dimensional integrals in Eqs. (20) and (21) can be reduced to the one-dimensional ones in the case of a spherically symmetric bare atomic potential and a spherically symmetric ground-state wave function, $V(\mathbf{r})=V(r)$, and $\psi_0(\mathbf{r})=\psi_0(r)$. Under these conditions both the spreading wave packet $\psi_0(\mathbf{r};t)$ and the effective potential $V_{\rm eff}(\mathbf{r};t)$ are spherically symmetric also. After integration over the angular variables Eq. (21) takes a form

$$\psi(r;t)=\left[\frac{-i}{2\pi t}\right]^{1/2}\frac{1}{r}\int_0^\infty dr'r'\psi_0(r')$$
$$\times\left\{\exp\left[\frac{(r-r')^2}{2t}\right]-\exp\left[\frac{(r+r')^2}{2t}\right]\right\}\ . \tag{22}$$

Similarly, under the same assumptions Eq. (19) for the effective potential reduces to

$$V_{\rm eff}(r;t)=\int_0^\infty dr'r'^2|\psi(r';t)|^2\int_{-1}^1 dx\ V((r^2+r'^2+2xrr')^{1/2})$$
$$=\frac{1}{2\pi t}\int_0^\infty dr'\int_{-1}^1 dx\ V((r^2+r'^2+2xrr')^{1/2})\left|\int_0^\infty dr''r''\psi_0(r'')\left\{\exp\left[\frac{(r''-r')^2}{2t}\right]-\exp\left[\frac{(r''+r')^2}{2t}\right]\right\}\right|^2 \tag{23}$$

and the effective force $\mathbf{F}_{\rm eff}(\mathbf{r};t)$ is directed along the vector $\mathbf{r}$

$$\mathbf{F}_{\rm eff}(\mathbf{r};t)=-\frac{\mathbf{r}}{r}\frac{\partial}{\partial r}V_{\rm eff}(r;t)\ . \tag{24}$$

In the specific case of the Coulomb bare atomic potential [$V(r)=-1/r$], Eqs. (23) and (24) can be simplified further to give

$$V_{\text{eff}}(r;t)=-2\left\{\frac{1}{r}\int_0^r dr'+\int_r^\infty\frac{dr'}{r'}\right\}r'^2|\psi(r';t)|^2$$
$$=-\frac{1}{\pi t}\left\{\frac{1}{r}\int_0^r dr'+\int_r^\infty\frac{dr'}{r'}\right\}\left|\int_0^\infty dr''r''\psi_0(r'')\left\{\exp\left[\frac{(r''-r')^2}{2t}\right]-\exp\left[\frac{(r''+r')^2}{2t}\right]\right\}\right|^2 \quad (25)$$

and

$$\mathbf{F}_{\text{eff}}(\mathbf{r};t)=-\frac{\mathbf{r}}{r}\frac{2}{r^2}\int_0^r dr'r'^2|\psi(r';t)|^2$$
$$=-\frac{\mathbf{r}}{r}\frac{1}{\pi t r^2}\int_0^r dr'\left|\int_0^\infty dr''r''\psi_0(r'')\left\{\exp\left[\frac{(r''-r')^2}{2t}\right]-\exp\left[\frac{(r''+r')^2}{2t}\right]\right\}\right|^2 . \quad (26)$$

The last result has a simple electrostatic interpretation. To see this, consider the atomic nucleus as a probe charge interacting with a spherically symmetric electron charge distribution by the Coulomb force. This probe charge is located at a distance r from the center of the electron charge distribution. In this case, as it is well known, due to the $1/r^2$ law of the Coulomb force there is a complete cancellation of contributions to the total force acting upon the probe charge from all the parts of the spherical electron charge distribution located outside the radius r from its center. In other words, the probe charge measures only that part of the electron charge distribution that is located inside the sphere with the radius r. This is the reason why the upper limit of integrations over r' in Eq. (25) is equal to r. It should be emphasized that this result is only valid for the Coulomb bare atomic potential (Coulomb forces) and a spherically symmetric initial and time-dependent field-free wave function $\psi(\mathbf{r};t)$. Without either of these assumptions, all parts of the electron distribution would give nonzero contributions to the effective force $\mathbf{F}_{\text{eff}}(\mathbf{r};t)$.

IV. MODELING OF THE GROUND-STATE ATOMIC WAVE FUNCTION AND BARE ATOMIC POTENTIAL; ONE- AND THREE-DIMENSIONAL PICTURES

In this section, the general expressions for $V_{\text{eff}}(\mathbf{r};t)$ and $\mathbf{F}_{\text{eff}}(\mathbf{r};t)$ will be analyzed and specified further in three and one dimensions for some reasonable and often used forms of the bare atomic potential and the ground-state atomic wave function.

A. Coulomb potential in three dimensions

For the Coulomb potential $V(r)=-1/r$, the hydrogen atom ground-state wave function is

$$\psi_0^{(H)}(\mathbf{r})=\frac{1}{\sqrt{\pi}}\exp(-r) . \quad (27)$$

However, to simplify the forthcoming analytical expressions it is convenient and reasonable to replace $\psi_0^{(H)}(\mathbf{r})$ by a Gaussian function

$$\psi_0^{(G)}(\mathbf{r})=\left[\frac{2}{\pi\Delta r_0^2}\right]^{3/4}\exp\left[-\left[\frac{r}{\Delta r_0}\right]^2\right] , \quad (28)$$

where Δr_0 is the initial size of the electron wave function $\psi_0(\mathbf{r})$. This size can be chosen, e.g., from the condition of the maximal overlapping of $\psi_0^{(G)}$ with $\psi_0^{(H)}$, that gives $\Delta r_0=1.92$ and provides an overlap of 97.8%. We have performed the forthcoming calculations for each of the ground-state representations, $\psi_0^{(G)}$ and $\psi_0^{(H)}$, and have found their results to differ only slightly.

After substituting $V(r)=-1/r$ and $\psi_0(\mathbf{r})=\psi_0^{(G)}(\mathbf{r})$ into Eqs. (22) and (25) we can perform all of the integrals and calculate explicitly the time-dependent field-free electron wave function $\psi(r;t)$ and the effective potential $V_{\text{eff}}(r;t)$. From Eq. (22) we get

$$|\psi(r;t)|^2=\left[\frac{2}{\pi[\Delta r(t)]^2}\right]^{3/2}\exp\left[-2\left[\frac{r}{\Delta r(t)}\right]^2\right] , \quad (29)$$

where

$$\Delta r(t)=\left[\Delta r_0^2+\frac{4t^2}{\Delta r_0^2}\right]^{1/2} . \quad (30)$$

Equation (29) describes the electron distribution of the spreading field-free Gaussian wave packet, where $\Delta r(t)$ is its time-dependent width. In accordance with Eq. (29), when the electron distribution $|\psi_0(\mathbf{r})|^2$ is initially determined by a Gaussian function of Eq. (28), the same shape characterizes the electron distribution at any time t, though with a growing width $\Delta r(t)$ [Eq. (30)].

By substituting $|\psi(r;t)|^2$ of Eq. (29) into Eq. (25) we find the effective potential

$$V_{\text{eff}}(r;t)=-\frac{1}{r}\text{erf}\left[\frac{r\sqrt{2}}{\Delta r(t)}\right] , \quad (31)$$

where erf denotes the error function [12]. Since for large arguments the error function approaches one, the effective potential $V_{\text{eff}}(r;t)$ coincides with the bare Coulomb potential $-1/r$ at large distances, $r\gg\Delta r(t)$. At small distances $r\ll\Delta r(t)$, $V_{\text{eff}}(r;t)$ of Eq. (31) approaches

$$V_{\text{eff}}(r;t)\approx V_{\text{eff}}(0;t)=-\frac{2\sqrt{2}}{\Delta r(t)\sqrt{\pi}} . \quad (32)$$

Thus, in contrast to the bare Coulomb potential, the effective potential $V_{\text{eff}}(r;t)$ has no singularity at $r=0$. As

mentioned before, the singularity is removed because the quantum-mechanical electron is a cloud, or a wave packet, rather than a classical point. This effect occurs at any t, beginning from the instant of time $t=0$ when the electron becomes free in accordance with the BSI assumption. As the time t increases, the magnitude of $V_{\rm eff}(0;t)$ decreases due to the WPS, and the width of the region of the smoothed singularity grows proportionally with $\Delta r(t)$. The dependence of $V_{\rm eff}(r;t)$ on r for three different instants of time t is shown in Fig. 2.

In accordance with Eq. (24), the derivative of $V_{\rm eff}(r;t)$ of Eq. (31) with respect to r yields the effective force

$$\mathbf{F}_{\rm eff}(\mathbf{r};t)=\frac{\mathbf{r}}{r^2}\left\{-\frac{1}{r}\,\mathrm{erf}\left[\frac{r\sqrt{2}}{\Delta r(t)}\right]+\frac{2^{3/2}}{\Delta r(t)\sqrt{\pi}}\times\exp\left[-2\left[\frac{r}{\Delta r(t)}\right]^2\right]\right\}. \tag{33}$$

The dependence of $F_{\rm eff}(r;t)$ on r is shown in Fig. 2(b) for several different instants of time t. As mentioned previously, the spherical symmetry of the electron density distribution causes the effective force to be zero at $r=0$, $F_{\rm eff}(0;t)=0$. At some electron-nucleus distance $r_0 \sim \Delta r(t)$, the force $F_{\rm eff}(r;t)$ has a minimum, and then, at larger r, it returns to zero following the long-range Coulomb law, $F_{\rm eff}(r;t)\sim -1/r^2$. The curve $F_{\rm eff}(r)$ grows smoother with time t, and its minimum becomes more shallow and located at larger distances r_0.

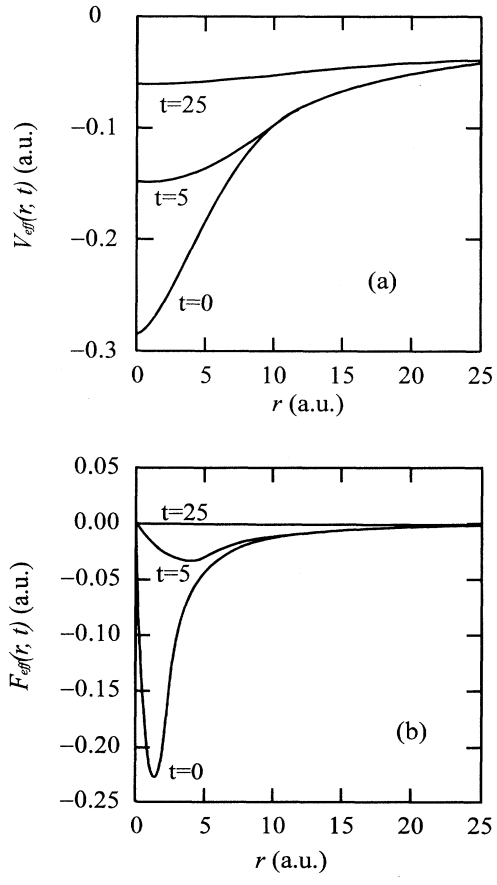

FIG. 2. (a) The effective atomic potential and (b) the Coulomb force on the wave packet at three different instants of time: $t=0$, $t=5$, and $t=25$. This calculation is based on the Gaussian model for the ground-state wave function [Eq. (28)].

It is interesting to compare the results derived above with those corresponding to the well-known Ehrenfest theorem [13,14]. This theorem describes a direct transition from the quantum-mechanical Schrödinger equation to the classical Newton equation. By using exact Schrödinger equation [Eq. (5)] and by calculating explicitly the second-order time derivative of the average electron position vector $\bar{\mathbf{r}}(t)\equiv\langle\Psi(\mathbf{r},t)|\mathbf{r}|\Psi(\mathbf{r},t)\rangle$ one can find an equation for $\bar{\mathbf{r}}(t)$:

$$\ddot{\bar{\mathbf{r}}}(t)=-\boldsymbol{\varepsilon}(t)-\langle\Psi(\mathbf{r},t)|\nabla V(\mathbf{r})|\Psi(\mathbf{r},t)\rangle\ . \tag{34}$$

In the general case, this equation is insufficient to describe $\bar{\mathbf{r}}(t)$ completely because the second term on the right-hand side is not determined by $\bar{\mathbf{r}}(t)$ alone. The only exception is that described by the Ehrenfest theorem which corresponds to the case when all quantum-mechanical corrections are small, i.e., the size of the localized wave function is small compared to the features of the potential. Then one can write $\mathbf{r}=\bar{\mathbf{r}}(t)+\delta\mathbf{r}$ and make the assumption that $|\delta\mathbf{r}|\ll|\bar{\mathbf{r}}(t)|$. In the zero-order approximation with respect to $\delta\mathbf{r}$, the second term on the right-hand side of Eq. (34) can be replaced by $-\nabla_{\bar{\mathbf{r}}}V(\bar{\mathbf{r}}(t))$, and Eq. (34) itself reduces to the Newton equation for $\bar{\mathbf{r}}(t)$ [Eq. (15)]. In this approximation, for example, the Coulomb potential conserves its singularity. In a sense, the results of the present work correspond to a case opposite to that described by the Ehrenfest theorem. In our case the quantum modification of the potential $V_{\rm eff}(\mathbf{r};t)$ as compared to $V(\mathbf{r})$ is not small. In particular the smoothing of the Coulomb singularity described above is a rather large effect, so the Ehrenfest theorem is inapplicable.

B. Smoothed Coulomb potential in one dimension

In the theory of strong-field laser-atom interaction, very often model 1D problems are considered instead of the real 3D one since 1D problems are much easier for numerical calculations. It is interesting to modify the 3D general theory described above to the 1D case, to see what effects dimensionality has on the model. By replacing all of the 3D integrals by the corresponding 1D ones in Eqs. (20) and (21) we can find immediately that in the 1D case the effective potential and force are given by

$$V_{\rm eff}(x;t)=\int dx' V(x+x')|\psi(x';t)|^2\ ,$$
$$F_{\rm eff}(x;t)=-\frac{\partial}{\partial x}V_{\rm eff}(x;t)\ , \tag{35}$$

where x is a single 1D coordinate, $-\infty<x<\infty$, and the field-free time-dependent electron distribution $|\psi(x';t)|^2$ has a form similar to that given by Eqs. (21)

$$\psi(x;t)=\left[\frac{-i}{2\pi t}\right]^{1/2}\int_{-\infty}^{\infty}dx'\exp\left[i\frac{(x-x')^2}{2t}\right]\psi(x';0)\ . \tag{36}$$

In the case of the singular 1D Coulomb potential $V(x)=-1/|x|$, the integral for the effective potential in Eq. (35) is divergent for any electron wave packet that is nonzero at the origin. Therefore, a direct consideration of the singular Coulomb interaction in the 1D model is senseless, at least under the BSI-WPS conditions discussed above. However, as has been the custom for 1D calculations [15], we can consider instead a smoothed, nonsingular potential such as

$$V(x)=-\frac{1}{\sqrt{2+x^2}}\ . \tag{37}$$

This potential has the same behavior for large values of x as the true Coulomb potential and has a ground state with the same binding energy as the ground state of the 3D Coulomb potential $E_0=0.5$. In addition, the ground state of this potential can be well approximated by the model Gaussian ground-state wave function

$$\psi(x;0)=\left[\frac{2}{\pi(\Delta x_0)^2}\right]^{1/4}\exp\left[-\frac{x^2}{(\Delta x_0)^2}\right], \tag{38}$$

where $\Delta x_0=2.65$ is chosen to provide the maximum overlap, 99.8%. For this potential and initial wave function Eqs. (35) and (36) yield for $V_{\rm eff}(x;t)$,

$$V_{\rm eff}(x;t)=-\frac{\sqrt{2}}{\sqrt{\pi}\Delta x'(t)}\int_{-\infty}^{\infty}dx'\frac{1}{\sqrt{2+x'^2}}\times\exp\left[-2\frac{(x'-x)^2}{[\Delta x(t)]^2}\right], \tag{39}$$

where $\Delta x(t)$ is the time-dependent width of the 1D wave packet similar to $\Delta r(t)$ in the 3D case [Eq. (30)]:

$$\Delta x(t)=\left[\Delta x_0^2+\frac{4t^2}{\Delta x_0^2}\right]^{1/2}. \tag{40}$$

In a sense, the artificially smoothed 1D potential of Eq. (37) is similar to the true Coulomb potential in the 3D picture since the 3D geometry inherently removes the singularity of the effective potential $V_{\rm eff}(x;t)$ as has been seen. However, the long-range Coulomb interaction causes the dipole acceleration to behave differently in 1D and 3D pictures as can be seen in Fig. 3. Figure 3 shows a comparison between the effective forces of the 1D model of Eq. (37) and the 3D model at the times t (typically within a single laser cycle) when the Gaussian wave packets of either picture have spread to a width $\Delta x=\Delta r=100$. While the force in either picture becomes less and less as the wave packets spread, the force in the 1D case decreases much more slowly than in the 3D case. This is because the 1D geometry overemphasizes the long-range Coulomb behavior.

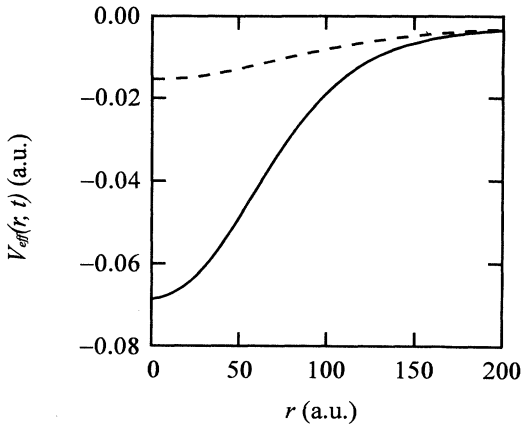

FIG. 3. The effective potentials for the smoothed 1D atomic potential (solid) and the exact 3D Coulomb potential (dotted). In each case the Gaussian electron wave packet has a width of $\Delta x=\Delta r=100$.

V. EMISSION OF LIGHT

The general results derived above can be used to describe emission of light by the electron in the BSI-WPS regime. It is known [16,17] that the Fourier spectrum of the dipole acceleration determines directly the coherent part of the emitted light spectral energy (i.e., the part proportional to the squared number density of the emitting atoms)

$$\left[\frac{d\mathcal{E}}{d\omega'}\right]_{\rm coh}\propto|(\ddot{\mathbf{d}})_{\omega'}|^2\ , \tag{41}$$

where ω' is the frequency of the emitted light, $d\mathcal{E}/d\omega'$ is the energy per unit interval of frequencies, and

$$(\ddot{\mathbf{d}})_{\omega'}=\int_0^{\infty}dt\,\ddot{\mathbf{d}}(t)\exp(i\omega' t)\ . \tag{42}$$

We now calculate the dipole acceleration $\ddot{\mathbf{d}}(t)$ and its Fourier transform $(\ddot{\mathbf{d}})_{\omega'}$ for some specific parameters of the laser pulse. The results of the calculations are shown in Figs. 4 and 5. Figure 4(a) shows the structure of the light pulse used, the dotted line is the time-dependent width of the wave packet $\Delta r(t)$ [Eq. (30)]. The time t is in optical cycles. The light frequency is chosen to be $\omega=0.5$, and the initial and peak values of the field amplitude $\varepsilon_0(t)$ are taken to be $\varepsilon_{0\rm in}\equiv\varepsilon_0(t=0)=0.0625$ and $\varepsilon_{0\rm max}=0.845$ (all in atomic units). These correspond to the initial and maximum values of the electron quiver motion amplitude of $\alpha_{0\rm in}\equiv\alpha_0(t=0)=25$ and $\alpha_{0\rm max}=338$. The pulse envelope is approximated by the Gaussian function $\varepsilon_0(t)=\varepsilon_{0\rm max}\exp[-(t-\Delta t)^2/\tau^2]$ with $\tau=3\times2\pi/\omega$ and $\Delta t=4.83\times2\pi/\omega$. The calculated dipole acceleration is shown in Fig. 4(b). The effective potential was calculated with the help of Eq. (31) in the model of the Gaussian ground-state wave function. The curve $\ddot{d}(t)$ of Fig. 4(b) shows a series of periodic kicks experienced by the oscillating electron as it returns to the nucleus. But the amplitudes of these kicks fall off very rapidly because of smoothing of the effective potential through WPS. The first kick not shown completely in Fig. 4(b) is in fact 200 times larger than the maximum value of $\ddot{d}(t)$ in the figure.

The aperiodicity of the dipole acceleration arising from

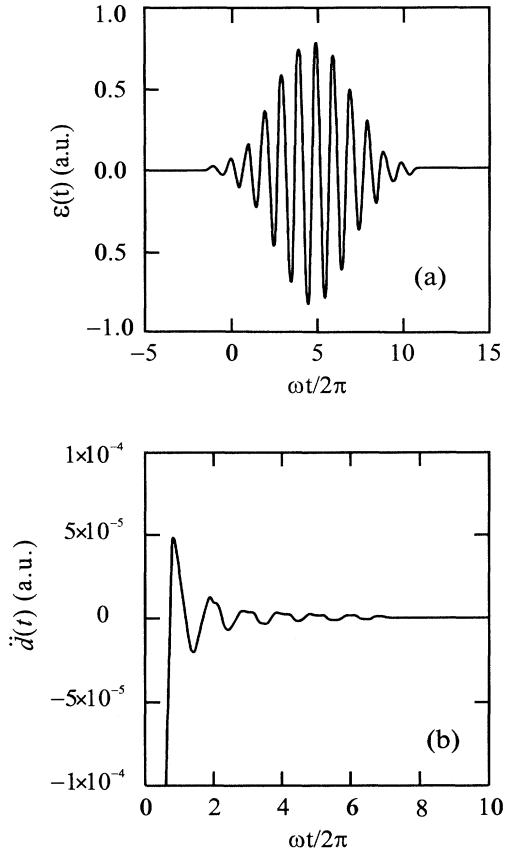

FIG. 4. The light pulse (a) and the dipole acceleration $\ddot{d}(t)$ (b) as a function of time t (in optical cycles).

the WPS strongly affects the spectrum of emission which is characterized by the squared absolute value of the Fourier transformed dipole acceleration [Eqs. (41) and (42)]. The result of the calculation is shown in Fig. 5. The spectrum of emission is wide with little structure. This is explained by the aperiodicity of the dipole acceleration in its dependence on the time t resulting from

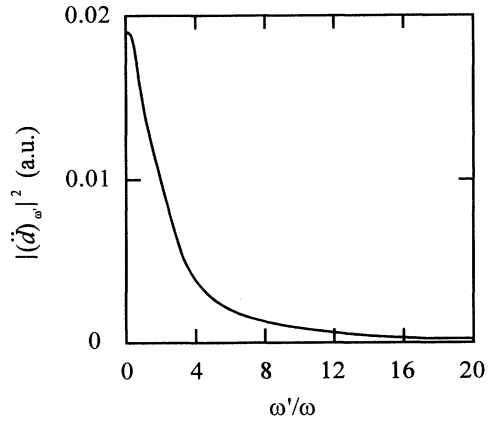

FIG. 5. Spectrum of the dipole acceleration $|(\ddot{\mathbf{d}})_{\omega'}|^2$ (in units of the laser frequency).

the WPS and the smoothing of the effective potential. In particular, the relatively large attraction felt by the electron wave packet as it leaves the atom for the first time has the greatest influence on the spectrum. In a macroscopic emitting media, harmonic structure can be carved out of the spectrum of Fig. 5 owing to the phase-matching effects. But for a microscopic emitting media with a perfect phase matching (i.e., all atoms emitting from a region much smaller than a wavelength) the emission spectrum arising under the BSI-WPS conditions shows no definite harmonics.

A comparison of this result with that of the theory based on the KFR approach [11] suggests that bound-free-bound atomic transitions are much more suitable for harmonic generation than coherent continuum-continuum transitions of an almost free electron. In other words, there is an optimum of the laser intensity for harmonic production. The field should be as strong as possible but not so strong that it destroys the atom so that the total probability of ionization per optical cycle is small. It is interesting to notice that there is a pronounced difference between the coherent case considered above and the case of spontaneous emission by external electrons scattered by a nucleus in the presence of a strong light field [18]. In the latter case, the harmonics do occur in the emission spectrum, and they become more emphasized with a stronger field. The explanation for this difference lies in the initial conditions: in the case considered in this paper the initial electron state is a localized wave packet that spreads, whereas in the case considered in Ref. [18] the incident (initial) electron state is a stationary plane wave. For this reason, WPS does not affect at all emission from a beam of external electrons but it does affect the emission of the electrons detached from the atoms by a strong laser field which collide again with their own parent ions.

VI. LIMITATIONS OF THE BSI-WPS MODEL

One of the main restrictions of the BSI-WPS model consists of a requirement mentioned above and found in Ref. [5] according to which the time-dependent width of the spreading wave packet has to be smaller than the double electron quiver motion amplitude. Assuming that the BSI conditions are fulfilled somewhere in the middle of the rise of the laser pulse, it is reasonable to require the formulated restriction to be valid up to the peak of the pulse envelope, i.e., up to $t \sim \tau$:

$$\Delta r(\tau) < 2\alpha_{0\max} , \tag{43}$$

where τ is the pulse duration, $\alpha_{0\max}$ denotes the quiver motion amplitude at the peak of the pulse envelope $\alpha_{0\max}=([\varepsilon_0(t)]_{\max}/\omega)^2$, and $\Delta r(\tau)$ is given by Eq. (30). Equation (43) determines the condition for which the atomic potential can be treated as a small perturbation. If this condition is not met $[\Delta r(\tau) > 2\alpha_{0\max}]$ then in accordance with Ref. [5] part of the electron density can be trapped by the atomic Kramers-Henneberger potential formed in a strong laser field, and this part does not behave any more as a free electron wave packet. For large times $\tau \gg 1$ (always the case), Eq. (30) gives

$\Delta r(\tau) \approx 2\tau/\Delta r_0$ and Eq. (43) can be considered as a limitation of the pulse duration τ

$$\tau < \alpha_{0\max} \Delta r \ . \tag{44}$$

This limitation can be rewritten in terms of the number N of optical cycles in the pulse,

$$N \equiv \frac{\omega\tau}{2\pi} < \alpha_{0\max}\omega \frac{\Delta r_0}{2\pi} \ . \tag{45}$$

The formulations throughout this paper have been based on the nonrelativistic approximation. This assumes in particular that the electron quiver motion velocity $\varepsilon_0(t)/\omega$ is much smaller than the speed of light $c = 137$, and hence the parameter $\alpha_{0\max}$ is limited by the condition

$$\alpha_{0\max}\omega < 137 \ . \tag{46}$$

All of the other limitations discussed below follow from the general condition that the electron does not acquire too large a drift during the action of the laser field. The drift can eliminate collisions with the parent nucleus completely, and this would change the picture described significantly. The drift was ignored above, but in reality there are several reasons for the drift to occur. For example, a drift can occur if the electron is born not exactly at an oscillation peak of the field ($t_0 \neq 0$). A drift can also arise from relativistic effects, and in particular the Lorenz force [5,19]. The latter can produce a significant drift even when the restriction of Eq. (46) is satisfied. We will analyze the limitations arising from the condition that the drift velocity caused by either of these mechanisms remains smaller than the rate of spreading $\Delta\dot{r}(t)$ where $\Delta r(t)$ is given by Eq. (30).

(i) The first drift mechanism is connected with the BSI assumptions. If the electron wave packet is detached from the atom not exactly at the peak of the field, it obtains an additional transversal drift velocity in the direction of $\boldsymbol{\varepsilon}$ equal to $v_\varepsilon(t_0) = [\varepsilon_0(t_0)/\omega]\sin(\omega t_0) = \alpha_{0\text{in}}\omega\sin(\omega t_0)$ where ωt_0 is a phase corresponding to the amount of time between the field oscillation peak ($t = 0$) and the moment of ionization t_0. The condition $v_\varepsilon(t_0) < \Delta\dot{r}(t)$ gives

$$\alpha_{0\text{in}}\omega|\sin(\omega t_0)| < 2/\Delta r_0 \ . \tag{47}$$

This restriction is not severe since for the parameters previously used ($\omega = 0.05, \alpha_{0\text{in}} = 25$, $\Delta r_0 = 1.92$), the inequality holds even when $\omega t_0 = \pi/4$.

(ii) The Lorenz-force drift velocity is equal to [5,19]

$$v_L(t) = \frac{[\varepsilon_0(t)]^2}{4c\omega^2} \ . \tag{48}$$

This drift can be ignored if $v_L(t)$ is less than $\Delta\dot{r}(t)$ which gives the condition

$$\alpha_{0\max}\omega < \left[\frac{8c}{\Delta r}\right]^{1/2} \sim 30 \ . \tag{49}$$

This restriction is stronger than that of Eq. (46). The condition of a small Lorenz-force drift [Eq. (49)] is compatible with the free WPS condition [Eqs. (43)–(45)] if the pulse is short enough, or if the number of optical cycles N is rather small,

$$N < \frac{\sqrt{2c\Delta r}}{\pi} \sim 5 \ . \tag{50}$$

Finally, it should be mentioned that under the formulated conditions the ponderomotive acceleration due to the inhomogeneous field of a laser focus does not provide significant drift because limitation of Eq. (50) requires the pulse to be much shorter than the time necessary for the electron to leave the focus [20]. The pulse used in the calculations of the emitted light spectrum in Sec. V is an example of one that meets all of the formulated conditions [Eqs. (45), (47), (49), and (50), plus the original BSI conditions of Eqs. (3) and (4)].

VII. CONCLUSION

We have calculated quantum mechanically the first-order correction to the electron dipole acceleration in the BSI-WPS model for electron detachment from an atom in a very strong laser field. The BSI-WPS assumptions are that the electron wave packet remains undistorted and attached to the atomic nucleus until the moment that the laser field suppresses the Coulomb barrier below the electron binding energy at which time the wave packet begins to execute free motion in the oscillating field as it spreads quantum mechanically. The first assumption, that of a clean and sudden break away by the electron wave packet from the nucleus, is perhaps the least tenable and is one that has not been addressed in this work. More likely, the wave packet leaves the vicinity of the nucleus with its shape significantly distorted with respect to the original bound state. In addition, it may be an extreme view to imagine that the entire wave packet leaves the nucleus in a single half laser cycle. Of course such distortions can strongly affect the details of the dipole acceleration and spectrum as calculated in this paper. Nevertheless, the qualitative features arising from wave packet spreading in this analysis should persist, and this is the primary justification for this work. These suggestions cannot be checked and clarified completely in the framework of the same approximations as used in this paper. They require an exact numerical *ab-initio* solution of the full Schrödinger equation [Eq. (5)], and we hope to return to this problem elsewhere.

Perhaps the most important result of the present work is that fast spreading of the detached electron wave packet strongly damps harmonic production. Very early (within a single laser cycle) after the electron wave packet begins to execute free motion in the field, it spreads to such a size that its acceleration due to the attraction to the parent ion is dramatically reduced as described in the first-order correction to free motion of the wave packet. This reduction of the dipole acceleration arising from the strong spreading can be intuitively understood electrostatically since the larger electron cloud is less attracted by the nucleus. The decline in the first-order correction to the dipole acceleration shows that the WPS assumption improves with time. For the same reason we can

conclude that high-order harmonic production occurs more readily for bound-bound or bound-continuum transitions as has been described in other models than for the continuum-continuum transitions that result from the scattering of the wave packet by the Coulomb potential. In this sense, perhaps this work can be thought as being complementary to the theory of harmonic emission based on the KFR approach which assesses bound-free-bound transitions while ignoring the free-free transitions [11]. In other words, we have analyzed that part of the problem that has been ignored and have found it to be an inefficient means of harmonic production. We know of no experiments that have examined the atomic emission in the regime where our theory should be valid.

It should be mentioned that the only case considered explicitly in this paper deals with ionization and emission from the ground atomic state, though the general equations derived above are valid for arbitrary initial wave functions and arbitrary bound atomic states. We expect that in the case of ionization and emission from a highly excited (Rydberg) level, the emission spectrum may have a much more pronounced structure (i.e., harmonic peaks) because the large size of Rydberg orbits causes the spreading of the corresponding wave packets to be much slower. As a result, the dipole acceleration $\ddot{\mathbf{d}}^{(0)}(t)$ should have a much more regular periodic dependence on time t than in the case of ionization from the ground state. This problem deserves its separate consideration.

ACKNOWLEDGMENTS

M.V. Fedorov acknowledges a support of the International Science Foundation (Grant No. M61000) and of the United States Army through its European Research Office (Grant No. N6817194C9001). J. Peatross acknowledges the support of the United States National Science Foundation through the Program for Long- and Medium-Term Research at Foreign Centers of Excellence (Grant No. INT-9302168).

[1] S. Augst, D. D. Meyerhofer, D. Strickland, and S. L. Chin, J. Opt. Soc. Am. B **8**, 858 (1991).
[2] S. Geltman and M. R. Teague, J. Phys. B **7**, L22 (1974).
[3] H. S. A. Neto and L. Davodovich, Phys. Rev. Lett. **53**, 2238 (1984).
[4] S. Geltman, Phys. Rev. A **43**, 4930 (1991).
[5] R. Grobe and M. V. Fedorov, Phys. Rev. Lett. **68**, 2592 (1992); Laser Phys. **3**, 265 (1993); J. Phys. B **26**, 1181 (1993).
[6] E. A. Volkova and A. M. Popov, Zh. Eksp. Teor. Fiz. **105**, 592 (1994) [Sov. Phys. JETP **78**, 315 (1994)].
[7] L. V. Keldysh, Zh. Eksp. Teor. Fiz. **45**, 1945 (1964) [Sov. Phys. JETP **20**, 1370 (1965)].
[8] F. H. M. Faisal, J. Phys. B **6**, L89 (1973).
[9] H. R. Reiss, Phys. Rev. **22**, 1786 (1980).
[10] H. A. Kramers, *Rapport du 8e Conseil Solvay, 1948* (Solvay Foundation, Brussels, 1950), p. 241; W. C. Henneberger, Phys. Rev. Lett. **21**, 838 (1968); M. Gavrila and J. Z. Kaminski, Phys. Rev. Lett. **52**, 613 (1984).
[11] M. Lewenstein, Ph. Balcou, M. Yu. Ivanov, A. L'Huillier, and P. B. Corkum, Phys. Rev. A **49**, 2117 (1994).
[12] I. S. Gradstein and I. M. Ryzhik, *Table of Integrals, Series and Products* (Academic, New York, 1980).
[13] A. S. Davidov, *Quantum Mechanics* (Pergamon, New York, 1976).
[14] A. Messiah, *Quantum Mechanics* (Wiley, New York, 1961), Vol. 1.
[15] Q. Su, J. H. Eberly, and J. Javanainen, Phys. Rev. Lett. **64**, 862 (1990).
[16] J. H. Eberly and M. V. Fedorov, Phys. Rev. A **45**, 4706 (1992).
[17] J. H. Eberly, D. Lappas, and M. V. Fedorov, Phys. Rev. A **47**, 1327 (1993).
[18] R. V. Karapetian and M. V. Fedorov, Zh. Eksp. Teor. Fiz. **75**, 816 (1978) [Sov. Phys. JETP **48**, 412 (1978)].
[19] T. Katsoules and W. B. Mori, Phys. Rev. Lett. **70**, 1561 (1993).
[20] R. R. Freeman *et al.*, Phys. Rev. Lett. **59**, 1092 (1987).